Aberrant inflammatory responses to type I interferon in STAT2 or IRF9 deficiency

Florian Gothe, MD,[a,b] Jarmila Stremenova Spegarova, PhD,[a] Catherine F. Hatton, MSc,[a] Helen Griffin, PhD,[a] Thomas Sargent, BSc,[a] Sally A. Cowley, PhD,[c] William James, DPhil,[c] Anna Roppelt, MD,[d] Anna Shcherbina, MD,[d] Fabian Hauck, MD, PhD,[b] Hugh T. Reyburn, PhD,[e] Christopher J. A. Duncan, DPhil,[a,f] and Sophie Hambleton, DPhil[a,g]

Newcastle, Newcastle upon Tyne, and Oxford, United Kingdom; Munich, Germany; Moscow, Russia; and Madrid, Spain

Background: Inflammatory phenomena such as hyperinflammation or hemophagocytic lymphohistiocytosis are a frequent yet paradoxical accompaniment to virus susceptibility in patients with impairment of type I interferon (IFN-I) signaling caused by deficiency of signal transducer and activator of transcription 2 (STAT2) or IFN regulatory factor 9 (IRF9).
Objective: We hypothesized that altered and/or prolonged IFN-I signaling contributes to inflammatory complications in these patients.
Methods: We explored the signaling kinetics and residual transcriptional responses of IFN-stimulated primary cells from individuals with complete loss of one of STAT1, STAT2, or IRF9 as well as gene-edited induced pluripotent stem cell–derived macrophages.
Results: Deficiency of any IFN-stimulated gene factor 3 component suppressed but did not abrogate IFN-I receptor signaling, which was abnormally prolonged, in keeping with insufficient induction of negative regulators such as ubiquitin-specific peptidase 18 (USP18). In cells lacking either STAT2 or IRF9, this late transcriptional response to IFN-α2b mimicked the effect of IFN-γ.
Conclusion: Our data suggest a model wherein the failure of negative feedback of IFN-I signaling in STAT2 and IRF9 deficiency leads to immune dysregulation. Aberrant IFN-α receptor signaling in STAT2- and IRF9-deficient cells switches the transcriptional output to a prolonged, IFN-γ–like response and likely contributes to clinically overt inflammation in these individuals. (J Allergy Clin Immunol 2022;150:955-64.)

Key words: *Type I interferon, antiviral immunity, ISGF3, HLH, type II interferon, GAF, STAT2, IRF9*

Interferons constitute an important and well-studied antiviral defense system in mammalian immunity.[1] Almost every human cell type is capable of both producing and responding to type I interferon (IFN-I; including various subtypes of IFN-α and IFN-β) in the face of viral challenge. Conversely, the production of type II interferon (IFN-γ), a potent immunostimulatory cytokine, is tightly regulated and confined to specific lymphocyte subsets. All IFNs, including the mucosa-restricted type III IFNs, use the Janus tyrosine kinase (JAK)-STAT pathway to influence gene expression. In the canonical model of signaling downstream of the IFN-α receptor (IFNAR), a heterotrimeric transcription factor complex is formed, consisting of tyrosine phosphorylated STAT1 and STAT2 together with IFN regulatory factor 9 (IRF9), and known as IFN-stimulated gene factor 3 (ISGF3). A fraction of phosphorylated STAT1, however, homodimerizes to form the IFN-γ activation factor (GAF), agonizing a partially overlapping set of IFN-stimulated genes (ISG), typically induced after type II IFN signaling via the IFN-γ receptor.[1] To restrain this potent proinflammatory response, robust negative feedback mechanisms are simultaneously induced by ISGF3 to terminate further IFNAR signaling. Failure of this negative feedback mechanism results in life-threatening IFN-mediated inflammatory disease.[2-5]

In recent years, severe virus susceptibility has been recognized as the shared clinical feature of monogenic inborn errors of IFN-I immunity resulting from biallelic deficiency of IFNAR, STAT1, STAT2, or IRF9.[6-9] In parallel, unexplained inflammatory phenotypes such as prolonged virus-induced or sterile hyperinflammation,[10] or even hemophagocytic lymphohistiocytosis (HLH),[9,11] have been noted in STAT2- and IRF9-deficient individuals, as in other defects of IFN-I immunity.[12-14] HLH is a state of severe, systemic hyperinflammation associated with excessive production of IFN-γ[15] and is often triggered by persistent virus

From [a]the Immunity and Inflammation Theme, Translational and Clinical Research Institute, Newcastle University, Newcastle; [b]the Department of Pediatrics, Dr von Hauner Children's Hospital, University Hospital, Ludwig-Maximilians-Universität Munich, Munich; [c]the James & Lillian Martin Centre for Stem Cell Research, Sir William Dunn School of Pathology, Oxford University, Oxford; [d]the Department of Immunology, Dmitry Rogachev National Medical Research Center of Pediatric Hematology, Oncology and Immunology, Moscow; [e]the Department of Immunology and Oncology, Spanish Center for Biotechnology (CNB-CSIC), Madrid; and [f]Infection and Tropical Medicine, Royal Victoria Infirmary, and [g]the Children's Immunology Service, Great North Children's Hospital, The Newcastle upon Tyne Hospitals NHS Foundation Trust, Newcastle upon Tyne.

The last 2 authors contributed equally to this article, and both should be considered senior author.

The Nanostring data set generated and analyzed during the current study is available from the corresponding author on request.

F. Gothe is supported by the Munich Clinician Scientist Program at LMU (FoeFoLe[plus]) and has received fellowships from the Bubble Foundation and the Care-for-Rare Foundation. C. F. Hatton is funded by an MRC studentship (MR/N013840/1). F. Hauck is funded by the Else Kröner-Fresenius Stiftung (EKFS, 2017_A110) and the German Federal Ministry of Education and Research (BMBF, 01GM1910C). S. Hambleton and C. J. A. Duncan are funded by the Wellcome Trust (207556/Z/17/Z and 211153/Z/18/Z respectively).

Disclosure of potential conflict of interest: S. Hambleton declares honoraria from CSL Behring and Takeda for teaching and consultancy. The rest of the authors declare that they have no relevant conflicts of interest.

Received for publication June 23, 2021; revised December 13, 2021; accepted for publication January 14, 2022.

Available online February 17, 2022.

Corresponding author: Sophie Hambleton, DPhil, or Christopher J. A. Duncan, DPhil, Translational and Clinical Research Institute, Immunity & Inflammation Theme, Faculty of Medical Sciences, 3rd Floor, Leech Building, Newcastle University Medical School, NE2 4HH, Newcastle upon Tyne, UK. E-mail: sophie.hambleton@ncl.ac.uk. Or: christopher.duncan@ncl.ac.uk.

The CrossMark symbol notifies online readers when updates have been made to the article such as errata or minor corrections

0091-6749

https://doi.org/10.1016/j.jaci.2022.01.026

Abbreviations used
CRISPR: Clustered regularly interspaced short palindromic repeats
EBV: Epstein-Barr virus
GAF: IFN-γ activation factor
GAS: IFN-γ activated sites
HLH: Hemophagocytic lymphohistiocytosis
ICAM1: Intercellular adhesion molecule 1
IFNAR: IFN-α receptor
IFN-I: Type I interferon
iPS: Induced pluripotent stem cell
IRF9: IFN regulatory factor 9
ISG: IFN stimulated gene
ISGF3: IFN-stimulated gene factor 3
JAK: Janus tyrosine kinase
KO: Knockout
LCL: Lymphoblastoid cell line
mRNA: Messenger RNA
p: Phosphorylated
PBS: Phosphate-buffered saline
SOCS: Suppressor of cytokine signaling
USP18: Ubiquitin-specific peptidase 18
WT: Wild type

replication in the face of an ineffective antiviral immune response. In the case of STAT2 and IRF9 deficiency, episodes of hyperinflammation have been reported in the absence of viral infection.[9,10]

Here, we consider the possibility that inflammation might arise in STAT2- or IRF9-deficient patients as a result of prolonged and/or altered IFNAR signaling. We provide evidence that aberrant IFNAR signaling in STAT2- and IRF9-deficient cells mimics the effects of IFN-γ stimulation, offering the potential for new therapeutic strategies in managing this life-threatening inflammatory state.

METHODS

The study was conducted according to the principles expressed in the Declaration of Helsinki and approved by the Newcastle and North Tyneside research ethics committee, as well as the institutional research ethics committees of LMU Munich, Dmitry Rogachev National Medical Research Moscow, and La Paz University Hospital.

Cells, cytokines, and inhibitors

Primary Epstein-Barr virus (EBV) lymphoblastoid cell lines (LCL) from a previously described patient with complete autosomal-recessive *STAT1* deficiency (p.V339Pfs*18),[13] an unreported patient with complete *STAT2* deficiency (compound heterozygous for 2 large deletions affecting *STAT2*: Chr12:56360796-Ch12:56352109 and Chr12:56355504-Ch12:56348082), and 2 siblings with complete *IRF9* deficiency (homozygous c.577+1G>T)[9] were cultured in RPMI 1640 medium supplemented by 10% fetal calf serum, 1% penicillin/streptomycin, and 1% L-glutamine (all from Gibco, Thermo Fisher Scientific, Waltham, Mass). Cytokines were used at the following concentrations: human recombinant IFN-α2b (1000 IU/mL; Intron A, Schering-Plough, Kennelworth, NJ), IFN-γ (1000 IU/mL; Immunikin, Boehringer Ingelheim, Ingelheim, Germany), IL-4 (50 ng/mL, PeproTech, London, United Kingdom), IL-5 (50 ng/mL, PeproTech), IL-13 (50 ng/mL, PeproTech), dexamethasone (10 μmol/L, Organon, Jersey City, NJ), and ruxolitinib (1 μmol/L, S1378, Calbiochem, San Diego, Calif).

Immunoblotting

A total of 10^6 EBV-LCL were washed in phosphate-buffered saline (PBS) and lysed on ice in lysis buffer [50 mmol Tris-HCl (pH 7.5), 150 mmol NaCl, 1% Nonidet P-40, 0.1% SDS, 0.5% Na-deoxycholate] containing 100 mmol dithiothreitol (Sigma-Aldrich, St Louis, Mo), 1× complete protease inhibitor cocktail (Roche, Basel, Switzerland), 1× PhosSTOP phosphatase inhibitors (Roche), and 1× NuPAGE Loading Buffer (Life Technologies, Carlsbad, Calif). Lysates were heated to 70°C for 10 minutes before being subjected to 4 to 12% Tris-glycine polyacrylamide gel (Novex, Life Technologies) electrophoresis in 1× SDS NuPAGE MOPS Running Buffer (Life Technologies) with Prestained Plus Protein Ladder (Thermo Fisher Scientific) as molecular weight markers. Proteins were transferred to 0.45 mm polyvinyl difluoride membranes (Thermo Fisher Scientific) in NuPAGE Tris-Glycine Transfer Buffer. Membranes were blocked for 60 minutes in 5% bovine serum albumin in Tris-buffered saline with 0.1% Tween before immunostaining by standard methods. A list of anti-human antibodies used together with appropriate horseradish peroxidase–conjugated secondary antibodies can be found in Table E1 in this article's Online Repository at www.jacionline.org. Membranes were washed in Tris-buffered saline with 0.1% Tween and developed with Immobilon Western Chemiluminescent horseradish peroxidase substrate (EMD Millipore, Billerica, Mass) and imaged on a LI-COR Odyssey Fc device (LI-COR, Lincoln, Neb).

Phospho-flow

A total of 2×10^5 EBV-LCL cells were seeded in 200 μL serum-free X-VIVO 15 medium (Lonza, Basel, Switzerland) and stimulated with IFN-α2b for the indicated times. In case a restimulation with IFN-γ was planned, cells were extensively washed to remove any IFN-α2b after the priming period, and cells were permitted to rest for 3 hours to allow pSTAT1 levels to return to baseline. After staining with Zombie UV (BioLegend, San Diego, Calif), cells were fixed using Cytofix buffer (BD Biosciences, Franklin Lakes, NJ). Permeabilization was achieved by adding ice-cold PermIII buffer (BD Biosciences), and cells were incubated on ice for 20 minutes. After repeated washing steps with PBS/2% fetal bovine serum, cells were stained for 60 minutes at room temperature with directly conjugated antibodies (see Table E2 in the Online Repository at www.jacionline.org). Samples were acquired on a Symphony A5 flow cytometer (BD Biosciences) and analyzed by FlowJo v10.2 software (Treestar, Ashland, Ore). The gating strategy can be found in Fig E1, *A,* in the Online Repository.

qRT-PCR analysis

For quantitative real-time PCR analysis, RNA was extracted using the ReliaPrep RNA Cell Miniprep System (Promega, Madison, Wisc), and equal amounts were reverse transcribed with Superscript III (Thermo Fisher Scientific). The resulting complementary DNA templates were subjected to quantitative PCR with a TaqManGene Expression Master Mix (Applied Biosystems, Thermo Fisher Scientific) according to the manufacturer's instructions. The primers and related probes we used were designed by Roche Universal Probe Library System Assay Design and are listed in Table E3 in the Online Repository at www.jacionline.org. Plates were run on an AriaMx Real-Time PCR System (Agilent Technologies, Santa Clara, Calif).

Immunoprecipitation

EBV-LCL were stimulated with IFN-α2b for 15 minutes, washed with ice-cold PBS, and lysed in RIPA buffer [50 mmol Tris (pH 7.5), 1 mmol EDTA, 150 mmol NaCl, 1% Nonidet P-40, 0.1% SDS, 0.5% Na-deoxycholate, 1× complete protease inhibitor cocktail (Roche), and 1× PhosSTOP phosphatase inhibitors (Roche)]. Lysates were centrifuged at 13,000 rpm at 4°C for 10 minutes. Soluble fractions were precleared for 1 hour at 4°C with Protein G Sepharose 4 Fast Flow beads (GE Healthcare, Chicago, Ill) that had been previously blocked with 1% bovine serum albumin containing wash buffer [50 mmol Tris (pH 7.5), 1 mmol EDTA, 150 mmol NaCl, 1% Nonidet P-40, 1× complete protease inhibitor cocktail (Roche), and 1× PhosSTOP phosphatase inhibitors (Roche)] for 1 hour. Precleared cell lysates were

immunoprecipitated overnight with blocked beads that were incubated with anti-STAT1a antibody (C-111) or anti-STAT2 antibody (A-7) for 1 hour and then washed 4 times in before boiling with 4× lithium dodecyl sulfate buffer at 95°C for 10 minutes to elute the absorbed immunocomplexes. Immunoblotting was carried out as described above.

Gene editing and induced pluripotent stem cell differentiation

The parental induced pluripotent stem cell (iPS) line (SFC856-03-04) used for clustered regularly interspaced short palindromic repeats (CRISPR) editing, which was generated from a healthy adult donor at the University of Oxford and has been described previously,[16] is registered in the Human Pluripotent Stem Cell Registry (https://hpscreg.eu/) and is available from the European Bank for Induced Pluripotent Stem Cells (https://ebisc.org/). For gene editing, the Alt-R CRISPR/Cas9 system [Integrated DNA Technologies (IDT), Coralville, Iowa] was used, with the aim to induce gene deletions that (1) remove exon–intron boundaries (for *STAT1* and *IRF9*) or (2) led to a frameshift (*STAT2*), thereby causing gene ablation through nonsense-mediated messenger RNA (mRNA) decay. The guide RNAs used are listed in Table E4 in the Online Repository at www.jacionline.org. To introduce guide RNAs alongside a tracrRNA as well as the Cas9 enzyme, the Neon transfection system (Thermo Fisher Scientific) was used. After transfection of the iPS pool, cells were plated at low density on irradiated mouse embryonic fibroblasts to allow single-cell colonies to grow. Individual colonies were selected with a microscope after 7 days and expanded in 96-well plates. The success of gene editing was assessed by immunoblot for STAT1 and STAT2. Because IRF9 is not expressed in iPS, clones were analyzed by nucleotide sequencing using the following primers: forward, TAGCGGTGCATGCCTGTAG; and reverse, AGCAAGGACAGAGGGTGAAG. The differentiation process was carried out following the protocol published by van Wilgenburg et al.[17] In brief, iPSs were seeded on AggreWell 800 plates (STEMCELL Technologies, Vancouver, British Columbia, Canada) at a density of 4×10^6/mL. Embryoid bodies were collected at day 4 and transferred into T175 flasks containing X-VIVO 15 medium (Lonza), supplemented with macrophage-colony stimulating factor (100 ng/mL) and IL-3 (25 ng/mL, both purchased from Invitrogen, Thermo Fisher Scientific). After several weeks of weekly media changes, macrophage precursors could be collected. These were plated at a density of 2×10^5 cells/mL and were terminally differentiated in X-VIVO 15 medium containing macrophage-colony stimulating factor in the above-mentioned concentration. After 7 days, macrophages were ready to be used for experiments. To confirm that the differentiated cells express key features of macrophages, analysis of different cell surface markers was assessed by flow cytometry, and a phagocytosis assay was carried out as described below. Additionally, STAT1, STAT2, and IRF9 were assessed by immunoblotting to ensure knockout (KO) of the specific protein.

Flow cytometry

Macrophages were lifted using PBS containing 5 mmol EDTA and washed with PBS/2% fetal calf serum. EBV-LCL were also washed using PBS/2% fetal calf serum. Cells were stained with surface markers for 30 minutes at room temperature. A list of directly conjugated antibodies can be found in Table E5 in the Online Repository at www.jacionline.org. To validate expression of various macrophage markers, appropriate isotype controls were used. When intracellular markers were investigated, cells were fixed using Cytofix buffer (BD Biosciences) and permeabilized with Cytoperm (BD Biosciences) according to the manufacturer's instructions. Intracellular staining was performed for 30 minutes at 4°C in the dark. Samples were acquired on a Symphony A5 flow cytometer (BD Biosciences) and analyzed by FlowJo v10.2 software. The gating strategy is exemplified in Fig E1, *A* and *B,* in the Online Repository.

Phagocytosis assay

A total of 2×10^5 macrophages were lifted and placed in Eppendorf tubes containing fresh X-VIVO 15 medium. pHrodo Red A Zymosan bioparticles (Invitrogen) were then added at a ratio of 10:1 cells. The negative control was immediately placed on ice, whereas the positive control was put into a shaking incubator for 2 hours at 37°C. Phagocytosis was terminated by placing the cells on ice. Macrophages were subsequently transferred to tubes for fluorescence-activated cell sorting, and 4′,6-diamidino-2-phenylindole (Thermo Fisher Scientific) was added before acquiring cells on a BD Biosciences Symphony Flow cytometer. Data were analyzed by FlowJo.

Cytokine production assay in macrophages

Macrophages were plated at a density of 2×10^5 cells/mL and preincubated with either IFN-α2b or IFN-γ at a concentration of 1000 IU/mL for 48 hours or left untreated. As a second stimulus, lipopolysaccharide was added at a final concentration of 100 ng/mL, and cells were further incubated for another 6 hours. Brefeldin A (BioLegend) was added to allow intracellular accumulation of cytokines under investigation. Cells were lifted using 5 mmol EDTA and stained with antibodies against TNF-α and IL-6.

Nanostring analysis

RNA was extracted by lysing macrophages in TRIzol reagent (Thermo Fisher Scientific) as previously described, then stored at −80°C until analysis. RNA was purified using the RNA Clean and Concentrator-5 kit (Zymo Research, Irvine, Calif) before 100 ng of total RNA was loaded onto the Nanostring nCounter cartridge following the manufacturer's instructions. Raw data files were imported into nSolver v4.0 software. All samples passed quality control assessment. Data normalization included positive control normalization as well as mRNA content normalization based on the expression of the housekeeping genes *ABCF1, GUSB, MRPS7, NMT1, NRDE2, OAZ1, PGK1, SDHA,* and *TBP.* Log_2-transformed expression or ratio data were exported and visualized by GraphPad Prism v9.0.2 software (GraphPad Software, La Jolla, Calif). Differentially expressed genes were analyzed for overrepresented conserved transcription factor binding sites in the promoter sequence (±10,000 bases) by single-site analysis using the oPOSSUM v3.0 database[18] with a conservation cutoff of 0.4 and matrix score threshold of 85%. Promoters were examined for the presence of ISGF3 (IFN-sensitive response element), IRF1, and STAT1 [IFN-γ activated site (GAS)] binding sites. For the pathway analysis, the ConsensusPathDB interaction database (http://consensuspathdb.org/)[19] was used to identify genes with significantly different expression after 48 hours of stimulation with IFN-α2b (1000 IU/mL). Genes were then referenced against the Gene Ontology (GO; http://geneontology.org/) resource[20] GO terms were ranked on the basis of their respective *Q* values compared to wild-type (WT) cells.

Statistical analysis

Unless otherwise stated, all experiments were repeated a minimum of 3 times. Data were normalized/$\log_{10}$ transformed before parametric tests of significance in light of the limitations of ascertaining distribution in small sample sizes and the high type II error rates of nonparametric tests in this context. Comparisons of more than 1 group used 1-way ANOVA with Tukey correction for multiple comparisons. Statistical testing was undertaken in GraphPad Prism v9.0.2. Two-tailed $P < .05$ was considered statistically significant.

RESULTS

Prolonged IFNAR signaling in ISGF3 component-deficient cells

We first examined the kinetics of IFNAR signaling by probing phosphorylation of JAK-STAT molecules in cells stimulated with IFN-I. Studies to date have focused on early events in ISGF3-deficient cells,[6-8] but here we sought to examine responses over a longer period, testing the prediction that defects in the induction of ISGF3-dependent negative regulation would lead to prolonged activation of the remaining JAK-STAT molecules. EBV-

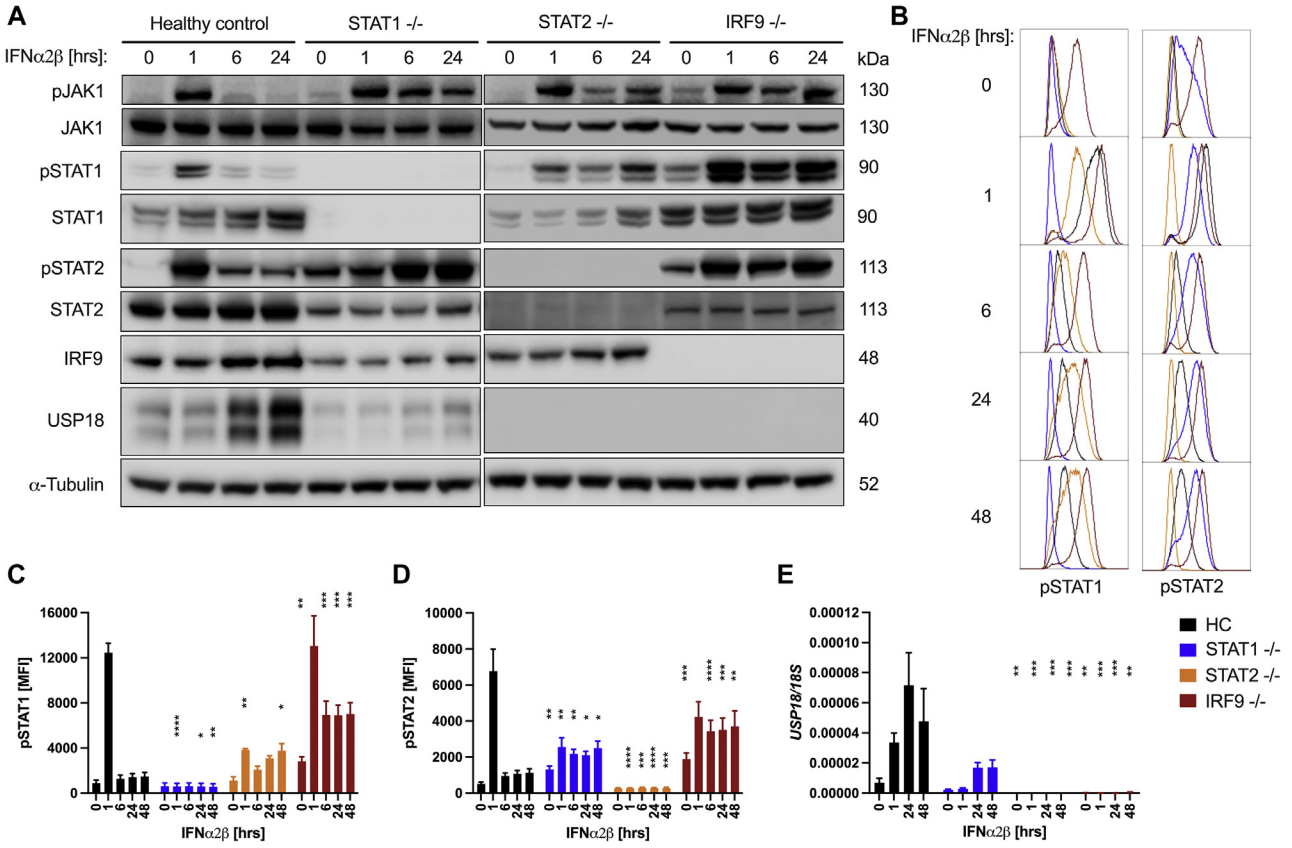

FIG 1. Prolonged IFNAR signaling and failure to upregulate USP18. Time course of IFN-α2b stimulation (1000 IU/mL) in EBV-LCL from patients and controls. (**A**) Immunoblot; repeat experiments n = 3. (**B**) Representative histograms (flow cytometry) with mean fluorescence intensity (MFI) of (**C**) pSTAT1 and (**D**) pSTAT2 over time; n = 4. (**E**) *USP18* mRNA expression over time measured by real-time reverse transcription–quantitative PCR; n = 3. Data are shown as means ± SEMs (**P* < .05, ***P* < .01, ****P* < .001, *****P* < .0001, 1-way ANOVA with Tukey correction for multiple comparisons).

transformed LCL were generated from patients with ISGF3-component deficiencies and stimulated with IFN-α2b for up to 48 hours (Fig 1). Immunoblotting confirmed that patient EBV-LCL were null for either STAT1, STAT2, or IRF9, and often showed secondarily reduced expression of other ISGF3 components at baseline (Fig 1, *A*). This is consistent with the fact that *STAT1, STAT2,* and *IRF9* are themselves ISGs, and their expression is positively regulated by "tonic" expression of IFN-I.[21] By contrast, JAK1 expression was preserved in ISGF3-deficient cells. In these EBV-transformed cell lines, we saw some evidence of basal IFN signaling in the form of constitutive phosphorylation of JAK1 and residual ISGF3 components (Fig 1, *A* and *B*).

After 1 hour of IFN-α2b stimulation, robust JAK1 phosphorylation was observed in healthy control cells as well as the different patient cell lines (Fig 1, *A*). However, the induction of STAT2 phosphorylation in STAT1$^{-/-}$ cells and pSTAT1 in STAT2$^{-/-}$ cells was significantly reduced at this early time point relative to control (Fig 1, *C* and *D*) as a result of reductions in total cellular STAT. In IRF9$^{-/-}$ cells, conversely, STAT1 and STAT2 were phosphorylated at similar levels as control cells. By 6 hours of stimulation, JAK1 phosphorylation was hardly visible in control cells (Fig 1, *A*), and both pSTAT1 and pSTAT2 had already decreased to levels only slightly above baseline (Fig 1, *C* and *D*), reflecting appropriate negative feedback on IFNAR. In marked contrast, JAK1 phosphorylation persisted in all ISGF3 component–deficient cells until at least 24 hours (Fig 1, *A*), indicative of persistent proximal signaling in the absence of ISGF3 components and the failure of negative feedback. Consistent with this, STAT2 phosphorylation remained elevated for up to 48 hours of stimulation in both STAT1$^{-/-}$ and IRF9$^{-/-}$ cells (Fig 1, *D*). A similar phenomenon was also seen in pSTAT1 levels in STAT2- or IRF9-deficient cells (Fig 1, *C*), and although both STAT2- and IRF9-deficient cells showed some degree of signal attenuation after 6 hours, pSTAT1 in STAT2$^{-/-}$ cells showed a secondary increase persisting to 48 hours. In IRF9$^{-/-}$ cells, pSTAT1 remained consistently elevated between 6 and 48 hours. In summary, IFN-α2b stimulation of cells lacking any ISGF3 component led to prolonged proximal signaling via IFNAR, albeit with differences in the kinetics and magnitude of STAT phosphorylation between the different deficient cell lines.

Failure of ubiquitin-specific peptidase 18–induced negative regulation

We hypothesized that prolonged IFNAR signaling might reflect a failure of negative feedback and proceeded to investigate the induction of relevant negative regulators. We focused on ubiquitin-specific peptidase 18 (USP18), which plays an essential role in suppressing IFN-I signaling[22] via displacement of JAK1 from IFNAR2 and prevention of

downstream phosphorylation. Whereas *USP18* mRNA expression peaked after 24 hours (Fig 1, *E*) in control cells, all ISGF3-deficient cell lines showed severely impaired *USP18* induction. Although some residual transcription was detectable in STAT1$^{-/-}$ cells, possibly reflecting the ability of residual STAT2:IRF9-containing complexes to mediate the expression of certain IFN-sensitive response element–containing ISGs in the absence of STAT1,[23,24] no induction of *USP18* could be observed in STAT2$^{-/-}$ or IRF9$^{-/-}$ cells, even as late as 48 hours after onset of IFN-α2b stimulation. We confirmed the preserved interaction of STAT2:IRF9 in STAT1$^{-/-}$ cells by immunoprecipitation (see Fig E2, *A,* in the Online Repository at www.jacionline.org). In contrast to previous reports,[25] STAT1 and IRF9 did not appear to interact in the absence of STAT2 when assessed by this method (Fig E2, *B*). The observed defect of USP18 induction on IFN-α2b stimulation was also evident at the protein level in STAT2- and IRF9-deficient cells (Fig 1, *A*). This biochemical phenotype recalls that seen in USP18-deficient cells[5] or cells with mutations in STAT2 that fail to support the regulatory action of USP18,[2,3] suggesting that defective USP18-dependent feedback was responsible for prolonged IFNAR signaling in ISGF3-deficient cells.

Members of the suppressor of cytokine signaling (SOCS) group of proteins are also capable of inhibiting JAK-STAT signaling by directly suppressing the JAK kinase domain,[26] although this activity fails to compensate for the loss of USP18 regulation in humans[2] or mice.[27] *SOCS1* and *SOCS3* are known to be potently induced on IFN stimulation[28] and indeed we saw preserved or even enhanced transcriptional induction of these regulators in ISGF3-component–deficient cells (see Fig E3, *A* and *B,* in the Online Repository at www.jacionline.org). This induction of *SOCS* expression led to functional regulatory activity on IFN-γ signaling in WT and IRF9-deficient cells (Fig E3, *C*), although pSTAT1 responses were generally attenuated in STAT2 deficiency (and absent in STAT1-deficient cells included as a negative control). Thus, although SOCS activity was induced in ISGF3-deficient cells, this did not compensate for the defect of negative regulation of IFNAR signaling.

GAS-dominated transcriptional output in STAT2$^{-/-}$ and IRF9$^{-/-}$ cells

Next, we investigated the transcriptional changes associated with such altered IFNAR signaling. As with expression of *USP18,* the induction of ISGs such as *MX1* (Fig 2, *A*), *RSAD2* (Fig 2, *B*), or *IFI44L* (Fig 2, *C*) was absent from all ISGF3-deficient cells, thus confirming that ISGF3 drives the typical transcriptional response to IFN-I, and in keeping with the virus susceptibility seen in these patients. In STAT2$^{-/-}$ and IRF9$^{-/-}$ cells, however, IFN-triggered formation of pSTAT1 homodimers, known as the gamma IFN activation factor (GAF), would be expected to be preserved. We therefore explored the transcriptional activation of genes harboring GAS elements. In keeping with our previous analysis, at 10 hours after IFN-α2b stimulation of STAT2-deficient cells,[7] we noted exaggerated induction of *IRF1* transcripts after 24 hours in both STAT2$^{-/-}$ and IRF9$^{-/-}$ cells (Fig 2, *D*). Extending our analysis to other classically IFN-γ–induced genes, we found increased transcription of *CIITA,* the master regulator of major histocompatibility complex class II expression in antigen-presenting cells, especially at later time points (Fig 2, *E*). The same was true for intercellular adhesion molecule 1 (*ICAM1*), encoding a protein expressed on macrophages and lymphocytes that facilitates cell–cell interaction including immune synapse formation (Fig 2, *F*). We confirmed the respective changes in the expression level of these markers after 48 hours of IFN-α2b stimulation (see Fig E4 in the Online Repository at www.jacionline.org).

Similar signaling kinetics in STAT2- and IRF9-KO macrophages

To confirm and extend our findings in a cell type more relevant to hyperinflammation *in vivo,* we used a model of macrophages derived from iPS. We used CRISPR/Cas9 technology to knock out *STAT1, STAT2,* or *IRF9* in a well-characterized iPS line, and selected gene-edited and isogenic WT control clones for experiments. These were differentiated to iPS macrophages using a well-defined protocol.[17] Analysis of the iPS macrophages confirmed successful KO of the respective ISGF3 component, but preserved expression of classical macrophage surface markers as well as phagocytic activity (Fig 3). Details of the differentiation protocol and functional validation can be found in the Methods as well as in Fig E5 in the Online Repository at www.jacionline.org.

Interestingly, the basal JAK-STAT phosphorylation observed in ISGF3-deficient EBV-LCL was absent from these untransformed cells. Stimulation with IFN-α2b for up to 48 hours induced similar kinetics of STAT phosphorylation, as seen in the EBV-LCL with prolonged activation of JAK1 and residual ISGF3 components. Again, we saw a complete lack of USP18 expression in STAT2$^{-/-}$ and IRF9$^{-/-}$ macrophages. Notably, some USP18 induction was observed in IFN-α2b–stimulated STAT1$^{-/-}$ cells, together with delayed and reduced expression of antiviral proteins MX1, RSAD2, and ISG15 (Fig 3, *A*), all of which were completely absent from STAT2- and IRF9-deficient cells. These data confirm earlier observations in EBV-LCL, consistent with reports that STAT2:IRF9 complexes mediate low-level ISG transcription in STAT1-deficient cells.[24]

Transcriptional changes in STAT2$^{-/-}$ and IRF9$^{-/-}$ macrophages reveal an IFN-γ–like pattern and altered time course

To profile transcriptional changes in stimulated KO iPS macrophages over time, we utilized the Nanostring Host Response Panel including 785 genes relevant to immune functions. Fig E6 in the Online Repository at www.jacionline.org displays differentially expressed genes at baseline, confirming the reduction in basal expression of several ISGs as a consequence of the loss of STAT2, IRF9, or STAT1. After 1 hour of IFN-α2b stimulation, all 3 KO lines displayed a marked failure to upregulate ISGs compared to WT cells, with STAT2$^{-/-}$ and IRF9$^{-/-}$ cells showing a strikingly similar pattern (Fig 4, *A*). Conversely, the response to IFN-γ was preserved in STAT2$^{-/-}$ and IRF9$^{-/-}$ cells, with STAT1$^{-/-}$ iPS macrophages serving as a negative control in this experimental setting (see Fig E7 in the Online Repository).

The previously observed failure of negative regulation became evident when comparing the transcriptional response at 1 and 48 hours of IFN-α2b stimulation (Fig 4, *B*). Whereas in WT cells most

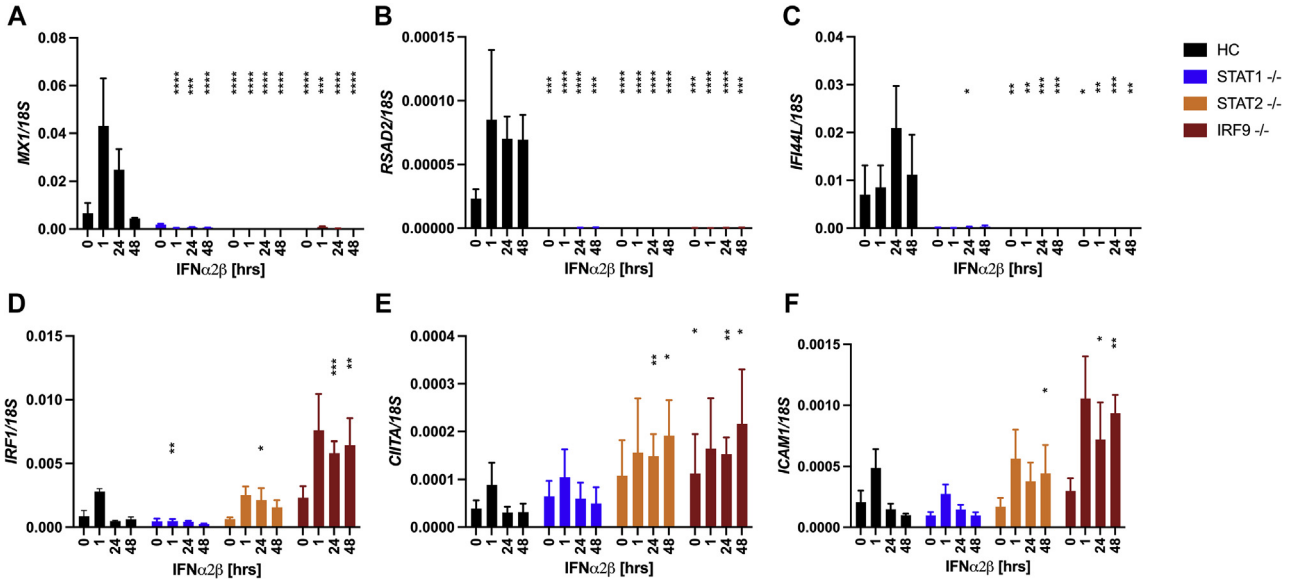

FIG 2. Failure to induce classical ISGs and heightened expression of GAS-controlled genes. Real-time reverse transcription–quantitative PCR analysis of ISGs in response to IFN-α2b stimulation (1000 IU/mL) for the indicated times. Expression of classical antiviral genes (**A**) *MX1,* (**B**) *RSAD2,* and (**C**) *IFI44L*. Induction of known IFN-γ–activated genes (**D**) *IRF1,* (**E**) *CIITA,* and (**F**) *ICAM1;* repeat experiments n = 3-4. Data are presented as means ± SEMs (**P* < .05, ***P* < .01, ****P* < .001, *****P* < .0001, 1-way ANOVA with Tukey correction for multiple comparisons).

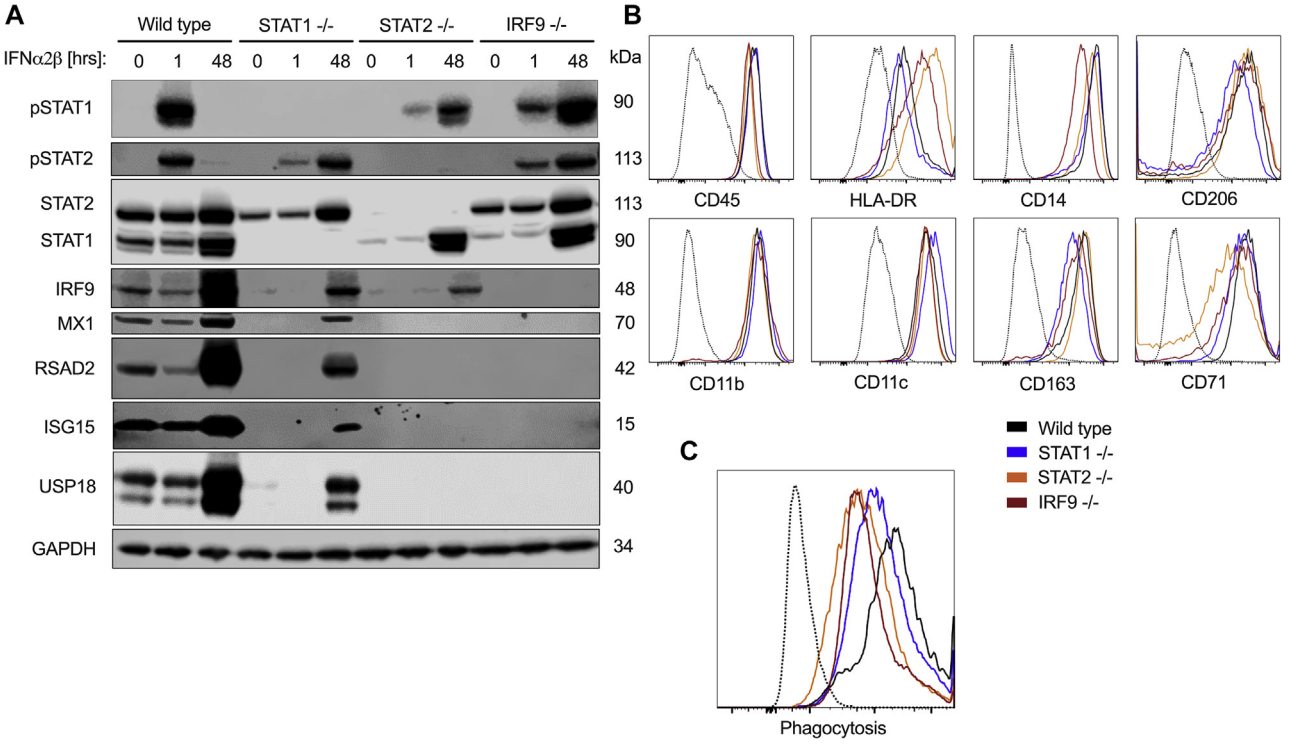

FIG 3. Validation of the iPS-derived KO macrophage lines. (**A**) Immunoblot of WT and KO iPS macrophage lines stimulated with IFN-α2b (1000 IU/mL) or left untreated; repeat experiments n = 3. (**B**) Representative flow cytometry histograms of iPS macrophage surface marker expression. *Dotted line* indicates isotype controls. (**C**) Phagocytosis assay comparing fluorescent bead uptake at 37°C vs 4°C (*dotted line,* negative control); repeat experiments n = 2.

of the initially upregulated genes show decreasing expression after 48 hours, STAT2$^{-/-}$ and IRF9$^{-/-}$ cells again showed a distinct pattern with a larger transcriptional response at the later time point. This delayed response to IFN-I was also qualitatively different in STAT2$^{-/-}$ and IRF9$^{-/-}$ iPS macrophages, with principal component analysis revealing the induction of an IFN-γ–like

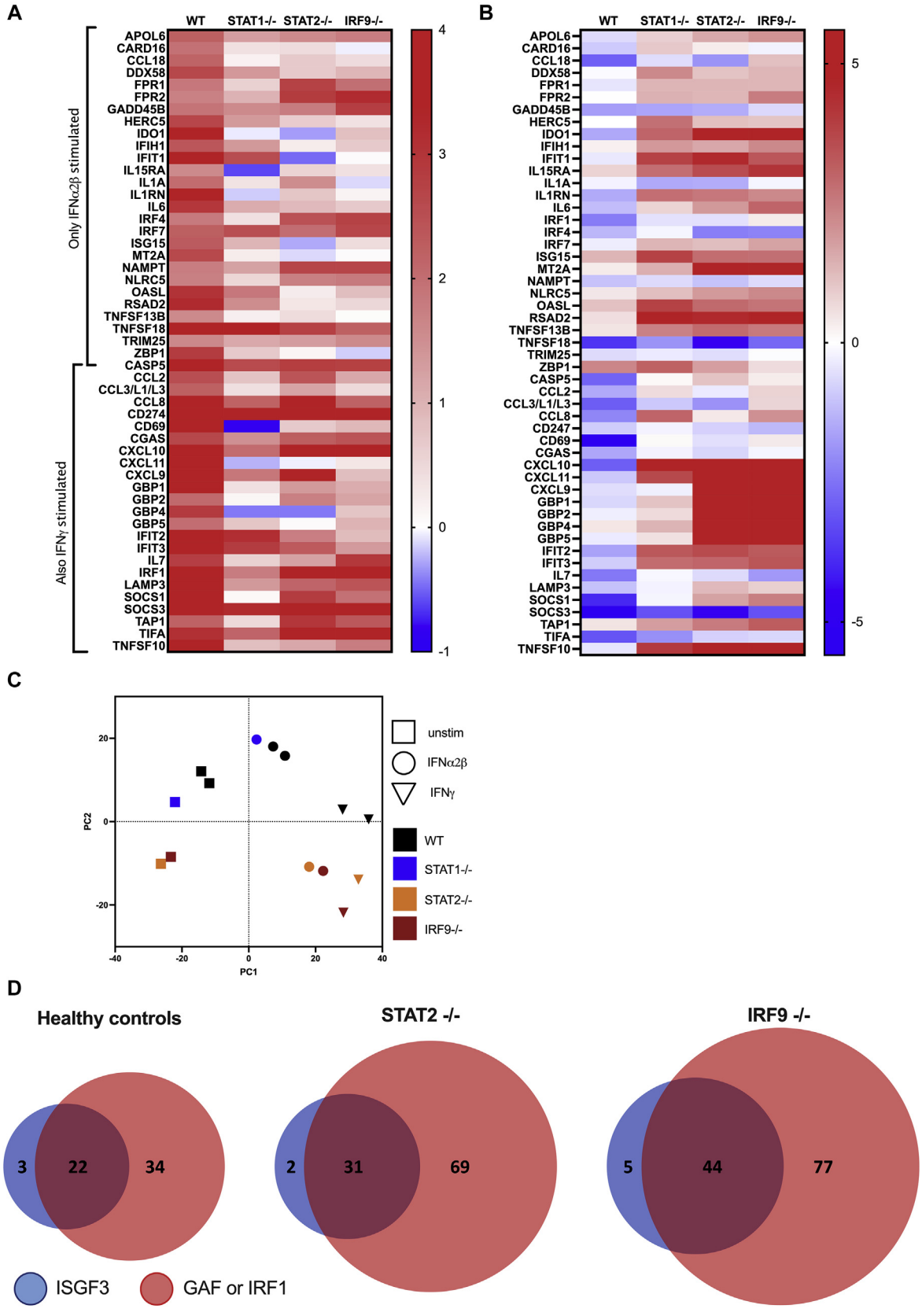

FIG 4. Transcriptional changes in iPS-derived KO macrophages after IFN stimulation. (**A**) ISG induction after IFN-α2b stimulation (1000 IU/mL) for 1 hour in WT, STAT1$^{-/-}$, STAT2$^{-/-}$, and IRF9$^{-/-}$ iPS macrophages on an isogenic background. Only the genes with >1.5-fold induction in both WT lines are displayed. (**B**) Fold changes between 1 and 48 hours of IFN-α stimulation analyzing the genes used in (*A*); $\log_2$ transformed data are shown. (**C**) Principal component analysis (PCA) analysis of samples after 48 hours of IFN-α2b or IFN-γ stimulation (1000 IU/mL each). PCA1 accounts for 46% of the variability, PCA2 for 19%; *square,* unstimulated; *circle,* IFN-α2b; *triangle,* IFN-γ. (**D**) Venn diagrams show numbers of differentially expressed genes with predicted binding sites for the indicated transcription factors ISGF3 or GAF and IRF1 within 1000 bp of their promoter sequence for WT, STAT2$^{-/-}$, and IRF9$^{-/-}$ iPS macrophages after 48 hours of IFN-α2b stimulation.

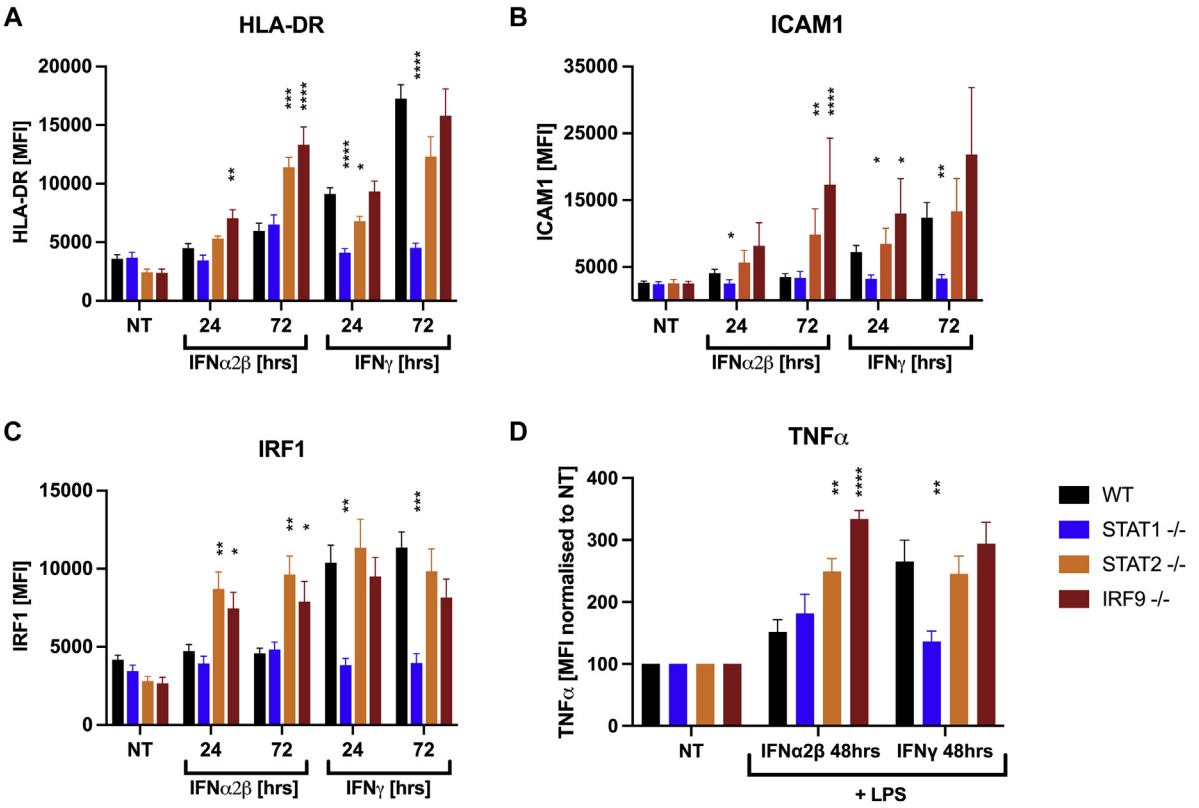

FIG 5. Macrophage activation in response to IFN stimulation. Upregulation of surface markers (**A**) HLA-DR, (**B**) ICAM1, and (**C**) IRF1 in iPS macrophages after stimulation with 1000 IU/mL IFN-α2b or IFN-γ. Repeat experiments n = 3. (**D**) Flow cytometric analysis of intracellular TNF-α accumulation. Cells were primed with IFN-α2b or IFN-γ for 48 hours before lipopolysaccharide (LPS; 100 ng/mL) was added as a second stimulus. Repeat experiments n = 3. Data are presented as means ± SEMs (*$P < .05$, **$P < .01$, ***$P < .001$, ****$P < .0001$, 1-way ANOVA with Tukey correction for multiple comparisons).

transcriptional profile (Fig 4, *C*). Analysis of the promoter regions of genes differentially expressed in STAT2$^{-/-}$ and IRF9$^{-/-}$ cells compared to WT after 48 hours of IFN-α2b stimulation revealed a trend toward enrichment of GAS or IRF1-binding motifs compared to WT cells (Fig 4, *D*). Accordingly, among the pathways upregulated in STAT2$^{-/-}$ and IRF9$^{-/-}$ iPS macrophages after 48 hours of IFN-α2b stimulation compared to WT were IFN-γ signaling, antigen processing and presentation, the immune response to tuberculosis, and proteasomal degradation, more typically associated with type II than IFN-I responses (see Fig E8 in the Online Repository at www.jacionline.org). Interestingly, WT and STAT1$^{-/-}$ responses to IFN-α2b grouped more closely on principal component analysis, which is in line with the immunoblot data showing preserved low-level induction of antiviral ISGs in the absence of STAT1 (Fig 3, *A*). We further profiled different cytokines implicated in HLH pathogenesis and observed increased transcription of *TNF, IL1B,* and *IL6* in STAT2-and IRF9-deficient cells (see Fig E9 in the Online Repository).

Increased macrophage activation and TNF-α production in STAT2$^{-/-}$ and IRF9$^{-/-}$ cells

To test whether the transcriptional shift toward an IFN-γ–like output translates to the protein level, and to consider the wider impact on macrophage activation, the upregulation of activation markers was assessed by flow cytometry (Fig 5). In control cells, IFN-α2b stimulation for either 24 or 72 hours did not affect expression levels of HLA-DR, ICAM1, or IRF1. With IFN-γ treatment, an increase over time was visible in all 3 of these markers (Fig 5, *A-C*). In STAT2$^{-/-}$ and IRF9$^{-/-}$ cells, however, IFN-α2b stimulation led to increased marker expression, comparable to that seen with IFN-γ stimulation of WT or mutant cells. As expected, STAT1$^{-/-}$ cells, used as a negative control, did not show substantial changes with either IFN-α2b or IFN-γ stimulation.

Furthermore, we assessed inflammatory cytokine production after priming macrophages with either IFN-α2b or IFN-γ for 48 hours, using lipopolysaccharide as the second stimulus (Fig 5, *D*). It has been well appreciated that IFN-γ primes macrophages for enhanced responsiveness to Toll-like receptor ligands and greatly augments Toll-like receptor–induced expression of inflammatory cytokines.[29] In both STAT2$^{-/-}$ and IRF9$^{-/-}$ macrophages, TNF-α production was increased to an equivalent degree after priming with either IFN-α2b or IFN-γ. This increased TNF-α production after IFN-α2b exposure mimicked IFN-γ responses in WT cells. IL-6 production, however, was not significantly enhanced in ISGF3 component–deficient iPS-derived macrophages over the levels in WT cells (see Fig E10 in the Online

Repository at www.jacionline.org). Interestingly, the upregulation of ICAM1, IRF1, and HLA-DR, also recapitulated in EBV-LCL, could be prevented by dexamethasone as well as ruxolitinib treatment but was unaffected by preexposure to T_H2 cytokines (see, respectively, Fig E11, *A-C,* and Fig E11, *D-F,* in the Online Repository).

DISCUSSION

In this study, we propose a contributary mechanism for hitherto unexplained inflammatory complications in STAT2$^{-/-}$ and IRF9$^{-/-}$ individuals. Besides the well-studied defect in initiating an antiviral state, our data indicate a delayed, altered, and dysregulated inflammatory response to IFN-I. Prolongation of ISGF3-independent IFNAR signaling, enabled by a failure to upregulate negative feedback inhibition via USP18, produces (1) a sustained shift toward GAF-driven transcription and (2) a functional state resembling a type II IFN response in macrophages, likely contributing to aberrant inflammation.

In healthy individuals, the inflammatory response to IFN-I is held in check by powerful negative feedback on proximal IFNAR signaling. A key finding of our studies in cells that lack ISGF3 components is that JAK-STAT activation in response to IFN-I is pathologically prolonged. A similar effect was previously described in mouse models of STAT1, STAT2, and IRF9 deficiency[30-32] and tentatively ascribed to insufficient early induction of *Socs1* transcription, known to interfere with Tyk2.[33] However, evidence including the clinical phenotype of their respective human deficiency states now indicates that USP18 plays the dominant role in negative regulation of IFNAR signaling.[5,34] USP18 is transcriptionally induced by ISGF3 and functions by sterically inhibiting the interaction of IFNAR2 and JAK1 in complex with STAT2.[22,35] Accordingly, mutations in *USP18* and *ISG15,* the latter of which functions in stabilizing USP18, have been found to cause type I interferonopathy by abrogating the downregulation of late IFN-I responses.[4,5] When USP18 function is inhibited as a consequence of perturbed interaction with STAT2, unrestrained IFN signaling is again observed.[2,3] Further experimental evidence corroborating the key role of USP18 is provided by Taylor et al[36]: in both human monocyte–derived macrophages where *USP18* has been knocked down as well as in iPS-derived macrophages with *USP18* KO, prolonged STAT1 and STAT2 signaling were observed after stimulation with IFN-I for 18 hours. The observed failure to robustly upregulate USP18 in STAT1$^{-/-}$, STAT2$^{-/-}$, and IRF9$^{-/-}$ cells is therefore likely sufficient to explain prolonged IFNAR signaling.

As well as this delayed time course, we observed a qualitatively altered macrophage transcriptional response to IFN-α2b in the context of STAT2 or IRF9 deficiency toward that produced by IFN-γ stimulation. This shift from IFN-I to IFN-II responses was reflected functionally in the heightened expression of macrophage activation markers such as IRF1, ICAM1, or HLA-DR, as well as increased production of TNF-α, a classical proinflammatory cytokine, which was comparable after IFN-α2b or IFN-γ in STAT2$^{-/-}$ and IRF9$^{-/-}$ macrophages. Consistent with our data, previous reports have described upregulation of major histocompatibility complex class II in *Stat2*$^{-/-}$ murine bone marrow–derived macrophages treated with IFN-α,[30] and adoption of an IFN-γ–like transcriptional state in IFN-α exposed *Stat2*$^{-/-}$ and *Irf9*$^{-/-}$ mixed glial cells.[32] Importantly, these IFN-I–dependent effects could be suppressed by treatment with dexamethasone, suggesting a potential therapeutic option in STAT2- or IRF9-deficient patients with hyperinflammation.

Our data confirm that the aberrant signaling shared by STAT2- and IRF9-deficient cells in response to IFN-I is distinct from STAT1-deficient cells—evidence that the switch to an IFN-γ–like transcriptional output is dependent on expression of STAT1. On the basis of our experiments in EBV-LCL, it is also tempting to conclude that there may be enhanced "tonic" IFNAR proximal signaling in IRF9, compared to STAT2 or STAT1, deficiency. However, when studies were conducted in (nontransformed) iPS macrophages, this phenotype was not observed. Furthermore, the basal transcriptome of STAT2$^{-/-}$ and IRF9$^{-/-}$ macrophages was indistinguishable. It remains to be determined whether apparent clinical differences in the inflammatory disease manifestations of IRF9 deficiency and STAT2 deficiency are mirrored by truly distinct molecular mechanisms.

An interesting aspect beyond the scope of this study is the transcriptional regulation in STAT1$^{-/-}$ cells, which we used mainly as a negative control for IFN-γ treatment. Although a complete ISGF3 complex cannot be formed in the absence of STAT1, the transcriptional profile of STAT1$^{-/-}$ macrophages treated with IFN-α2b was qualitatively similar to that of WT cells, and some expression of antiviral proteins like MX1, RSAD2, and ISG15 was noted. In murine *Stat1*$^{-/-}$ bone marrow–derived macrophages, a similar delayed upregulation of *MX1* and *ISG15* transcripts, absent from STAT2- and IRF9-deficient cells, has been noted[31] and attributed to a complex of IRF9 and STAT2 that can bind a subset of IFN-sensitive response element sites.[24,37] Furthermore, retained although low-level USP18 expression in our STAT1$^{-/-}$ cells is consistent with residual negative regulation of IFNAR signaling despite the lack of ISGF3. Nevertheless, inflammatory disease manifestations fulfilling HLH criteria have also been recognized in STAT1 deficiency[38] as well as IFNAR1[14] and IFNAR2[39] deficiency states, clearly arguing for the involvement of signaling cascades other than IFN-I in the pathogenesis of HLH.

In summary, our data clearly demonstrate unrestrained and aberrant IFNAR signaling in STAT2$^{-/-}$ and IRF9$^{-/-}$ cells in response to IFN-α2b. IFN-I is induced in response to viral infection or vaccination with live attenuated virus, and it contributes to innate immune antiviral restraint. Failure to contain virus replication—well documented, for example, in STAT2 deficiency[10]—might provoke excessive and prolonged IFN-I production, in turn driving aberrant IFN-γ–like inflammatory responses. Although paradoxical at first sight, our data suggest the potential use of JAK inhibitors to terminate the dysregulated IFN-I response in order to limit immunopathology in this subgroup, as in other patients with HLH.[40]

We thank Angela Grainger (Immunity and Inflammation Theme, Translational and Clinical Research Institute, Newcastle University, Newcastle, United Kingdom) for excellent technical assistance as well as Cathy Browne (James & Lillian Martin Centre for Stem Cell Research, Sir William Dunn School of Pathology, Oxford University, Oxford, United Kingdom) for expert assistance with iPS cell culture.

Key messages

- **Cells deficient in components of the ISGF3 transcription factor complex (STAT1, STAT2, IRF9) display prolonged IFNAR signaling as a consequence of failure to initiate negative feedback regulation via USP18.**
- **In STAT2$^{-/-}$ and IRF9$^{-/-}$ cells, this dysregulated response leads to a sustained shift toward STAT1-dependent transcription, inducing in macrophages a functional state more closely resembling an IFN-γ response.**
- **This aberrant inflammatory response provides an explanation for the clinical manifestations of hyperinflammation seen in patients with autosomal recessive deficiency of *STAT2* and *IRF9*.**

REFERENCES

1. Duncan CJA, Randall RE, Hambleton S. Genetic lesions of type I interferon signalling in human antiviral immunity. Trends Genet 2021;37:46-58.
2. Duncan CJA, Thompson BJ, Chen R, Rice GI, Gothe F, Young DF, et al. Severe type I interferonopathy and unrestrained interferon signaling due to a homozygous germline mutation in STAT2. Sci Immunol 2019;4:eaav7501.
3. Gruber C, Martin-Fernandez M, Ailal F, Qiu X, Taft J, Altman J, et al. Homozygous STAT2 gain-of-function mutation by loss of USP18 activity in a patient with type I interferonopathy. J Exp Med 2020;217:1-11.
4. Zhang X, Bogunovic D, Payelle-Brogard B, Francois-Newton V, Speer SD, Yuan C, et al. Human intracellular ISG15 prevents interferon-α/β over-amplification and auto-inflammation. Nature 2015;517(7532):89-93.
5. Meuwissen MEC, Schot R, Buta S, Oudesluijs G, Tinschert S, Speer SD, et al. Human USP18 deficiency underlies type 1 interferonopathy leading to severe pseudo-TOR CH syndrome. J Exp Med 2016;213:1163-74.
6. Dupuis S, Jouanguy E, Al-Hajjar S, Fieschi C, Zaid Al-Mohsen I, Al-Jumaah S, et al. Impaired response to interferon-α/β and lethal viral disease in human STAT1 deficiency. Nat Genet 2003;33:388-91.
7. Hambleton S, Goodbourn S, Young DF, Dickinson P, Mohamad SMB, Valappil M, et al. STAT2 deficiency and susceptibility to viral illness in humans. Proc Natl Acad Sci U S A 2013;110:3053-8.
8. Hernandez N, Melki I, Jing H, Habib T, Huang SSY, Danielson J, et al. Life-threatening influenza pneumonitis in a child with inherited IRF9 deficiency. J Exp Med 2018;215:2567-85.
9. Bravo García-Morato M, Calvo Apalategi A, Bravo-Gallego LY, Blázquez Moreno A, Simón-Fuentes M, Garmendia JV, et al. Impaired control of multiple viral infections in a family with complete IRF9 deficiency. J Allergy Clin Immunol 2019;144:309-12.e10.
10. Moens L, Van Eyck L, Jochmans D, Mitera T, Frans G, Bossuyt X, et al. A novel kindred with inherited STAT2 deficiency and severe viral illness. J Allergy Clin Immunol 2017;139:1995-7.e9.
11. Alosaimi MF, Maciag MC, Platt CD, Geha RS, Chou J, Bartnikas LM. A novel variant in STAT2 presenting with hemophagocytic lymphohistiocytosis. J Allergy Clin Immunol 2019;144:611-3.e3.
12. Burns C, Cheung A, Stark Z, Choo S, Downie L, White S, et al. A novel presentation of homozygous loss-of-function STAT-1 mutation in an infant with hyperinflammation—a case report and review of the literature. J Allergy Clin Immunol Pract 2016;4:777-9.
13. Boehmer DFR, Koehler LM, Magg T, Metzger P, Rohlfs M, Ahlfeld J, et al. A novel complete autosomal-recessive STAT1 LOF variant causes immunodeficiency with hemophagocytic lymphohistiocytosis-like hyperinflammation. J Allergy Clin Immunol Pract 2020;8:3102-11.
14. Gothe F, Hatton CF, Truong L, Klimova Z, Kanderova V, Fejtkova M, et al. A novel case of homozygous interferon alpha/beta receptor alpha chain (IFNAR1) deficiency with hemophagocytic lymphohistiocytosis. Clin Infect Dis 2022;74:136-9.
15. Jordan MB, Hildeman D, Kappler J, Marrack P. An animal model of hemophagocytic lymphohistiocytosis (HLH): CD8^{+} T cells and interferon gamma are essential for the disorder. Blood 2004;104:735-43.
16. Haenseler W, Zambon F, Lee H, Vowles J, Rinaldi F, Duggal G, et al. Excess α-synuclein compromises phagocytosis in iPSC-derived macrophages. Sci Rep 2017;7:1-11.
17. van Wilgenburg B, Browne C, Vowles J, Cowley SA. Efficient, long term production of monocyte-derived macrophages from human pluripotent stem cells under partly-defined and fully-defined conditions. PLoS One 2013;8:e71098.
18. Ho Sui SJ, Mortimer JR, Arenillas DJ, Brumm J, Walsh CJ, Kennedy BP, et al. oPOSSUM: identification of over-represented transcription factor binding sites in co-expressed genes. Nucleic Acids Res 2005;33:3154-64.
19. Kamburov A, Stelzl U, Lehrach H, Herwig R. The ConsensusPathDB interaction database: 2013 update. Nucleic Acids Res 2013;41(D1):793-800.
20. Carbon S, Douglass E, Good BM, Unni DR, Harris NL, Mungall CJ, et al. The Gene Ontology resource: enriching a GOld mine. Nucleic Acids Res 2021;49(D1):D325-34.
21. Gough DJ, Messina NL, Clarke CJP, Johnstone RW, Levy DE. Constitutive type i interferon modulates homeostatic balance through tonic signaling. Immunity 2012;36:166-74.
22. Malakhova OA, Kim K Il, Luo JK, Zou W, Kumar KGS, Fuchs SY, et al. UBP43 is a novel regulator of interferon signaling independent of its ISG15 isopeptidase activity. EMBO J 2006;25:2358-67.
23. Platanitis E, Demiroz D, Schneller A, Fischer K, Capelle C, Hartl M, et al. A molecular switch from STAT2-IRF9 to ISGF3 underlies interferon-induced gene transcription. Nat Commun 2019;10:2921.
24. Blaszczyk K, Olejnik A, Nowicka H, Ozgyin L, Chen YL, Chmielewski S, et al. STAT2/IRF9 directs a prolonged ISGF3-like transcriptional response and antiviral activity in the absence of STAT1. Biochem J 2015;466:511-24.
25. Majumder S, Zhou LZ, Chaturvedi P, Babcock G, Aras S, Ransohoff RM. p48/STAT-1alpha-containing complexes play a predominant role in induction of IFN-gamma–inducible protein, 10 kDa (IP-10) by IFN-gamma alone or in synergy with TNF-alpha. J Immunol 1998;161:4736-44.
26. Kershaw NJ, Murphy JM, Liau NPD, Varghese LN, Laktyushin A, Whitlock EL, et al. SOCS3 binds specific receptor-JAK complexes to control cytokine signaling by direct kinase inhibition. Nat Struct Mol Biol 2013;20:469-76.
27. Goldmann T, Zeller N, Raasch J, Kierdorf K, Frenzel K, Ketscher L, et al. USP 18 lack in microglia causes destructive interferonopathy of the mouse brain. EMBO J 2015;34:1612-29.
28. Song MM, Shuai K. The suppressor of cytokine signaling (SOCS) 1 and SOCS3 but not SOCS2 proteins inhibit interferon-mediated antiviral and antiproliferative activities. J Biol Chem 1998;273:35056-62.
29. Qiao Y, Giannopoulou EG, Chan CH, ho Park S, Gong S, Chen J, et al. Synergistic activation of inflammatory cytokine genes by interferon-γ–induced chromatin remodeling and Toll-like receptor signaling. Immunity 2013;39:454-69.
30. Zhao W, Cha EN, Lee C, Park CY, Schindler C. Stat2-dependent regulation of MHC class II expression. J Immunol 2007;179:463-71.
31. Abdul-Sater A, Majoros A, Plumlee1 C, Perry S, Gu A, Lee C, et al. Different STAT transcription complexes drive early and delayed responses to type I interferons. J Immunol 2015;195:210-6.
32. Li W, Hofer MJ, Songkhunawej P, Jung SR, Hancock D, Denyer G, et al. Type I interferon–regulated gene expression and signaling in murine mixed glial cells lacking signal transducers and activators of transcription 1 or 2 or interferon regulatory factor 9. J Biol Chem 2017;292:5845-59.
33. Piganis RAR, De Weerd NA, Gould JA, Schindler CW, Mansell A, Nicholson SE, et al. Suppressor of cytokine signaling (SOCS) 1 inhibits type I interferon (IFN) signaling via the interferon α receptor (IFNAR1)-associated tyrosine kinase tyk2. J Biol Chem 2011;286:33811-8.
34. Hadjadj J, Castro CN, Tusseau M, Stolzenberg MC, Mazerolles F, Aladjidi N, et al. Early-onset autoimmunity associated with SOCS1 haploinsufficiency. Nat Commun 2020;11:1-11.
35. Arimoto KI, Miyauchi S, Stoner SA, Fan JB, Zhang DE. Negative regulation of IFN-I signaling. J Leukoc Biol 2018;103:1099-116.
36. Taylor JP, Cash MN, Santostefano KE, Nakanishi M, Terada N, Wallet MA. CRISPR/Cas9 knockout of USP18 enhances IFN-I responsiveness and restricts HIV-1 infection in macrophages. J Leukoc Biol 2018;103:1225-40.
37. Bluyssen HAR, Levy DE. Stat2 is a transcriptional activator that requires sequence-specific contacts provided by Stat1 and p48 for stable interaction with DNA. J Biol Chem 1997;272:4600-5.
38. Le Voyer T, Sakata S, Tsumura M, Khan T, Esteve-Sole A, Al-Saud BK, et al. Genetic, immunological, and clinical features of 32 patients with autosomal recessive STAT1 deficiency. J Immunol 2021;207:133-52.
39. Passarelli C, Civino A, Rossi MN, Cifaldi L, Lanari V, Moneta GM, et al. *IFNAR2* deficiency causing dysregulation of NK cell functions and presenting with hemophagocytic lymphohistiocytosis. Front Genet 2020;11:937.
40. Chinn IK, Eckstein OS, Peckham-Gregory EC, Goldberg BR, Forbes LR, Nicholas SK, et al. Genetic and mechanistic diversity in pediatric hemophagocytic lymphohistiocytosis. Blood 2018;132:89-100.

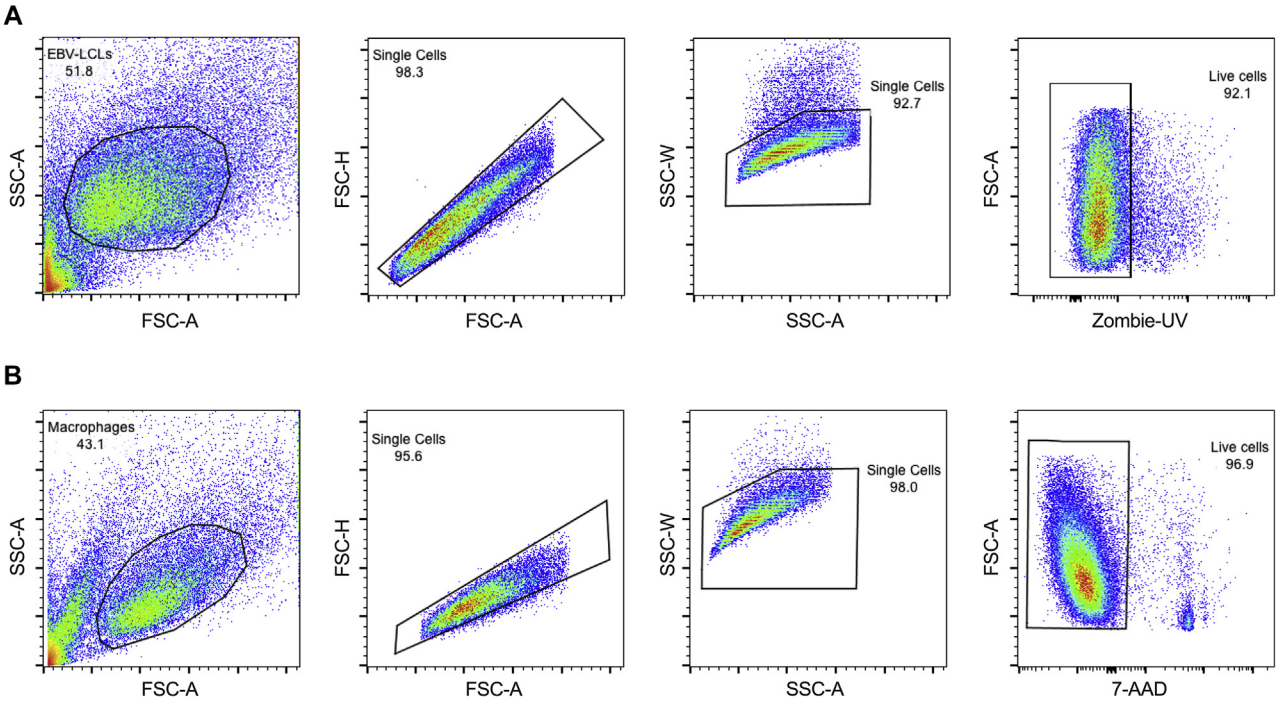

FIG E1. Gating strategies in (**A**) EBV-LCL and (**B**) iPS-derived macrophages.

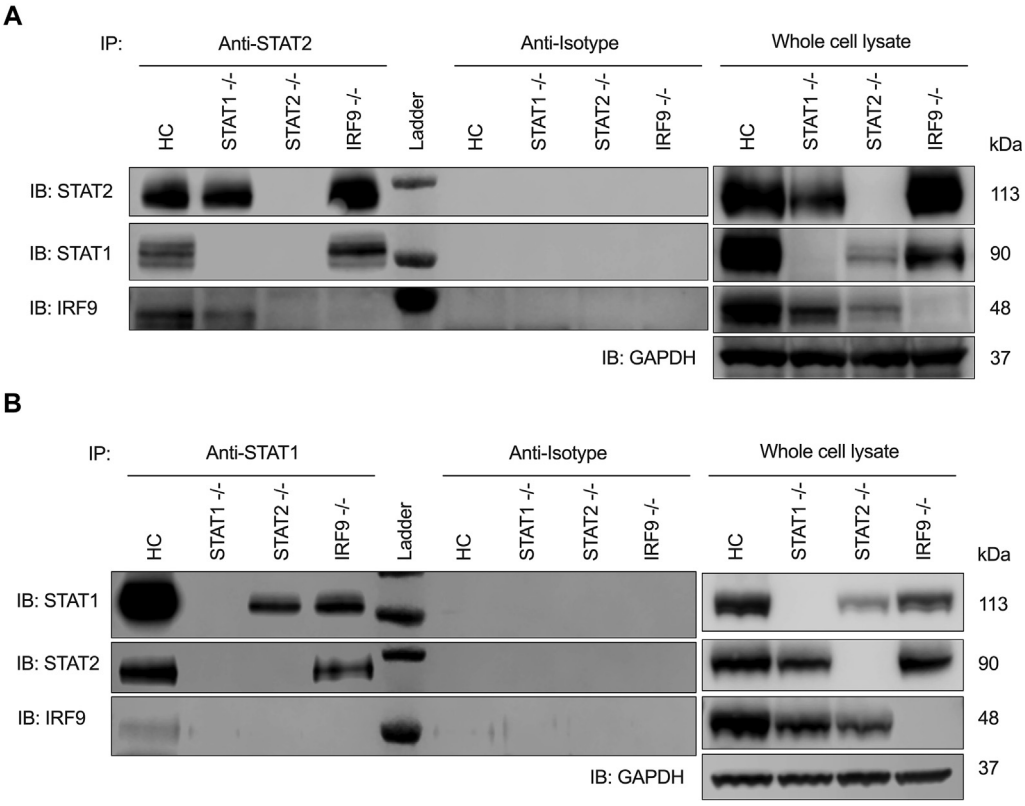

FIG E2. Coimmunoprecipitation of (**A**) STAT1 and (**B**) STAT2 in EBV-LCL stimulated with IFN-α2b (1000 IU/mL) for 15 minutes. Representative images from 3-4 independent experiments.

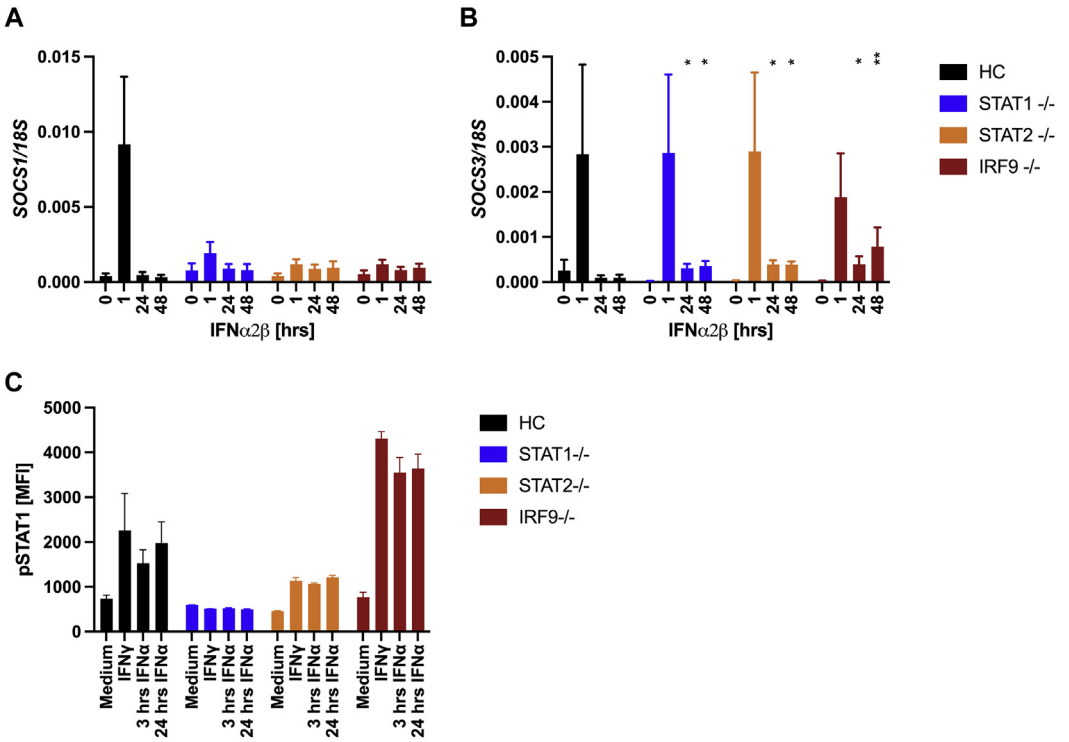

FIG E3. Real-time reverse transcription–quantitative PCR analysis of (**A**) *SOCS1* and (**B**) *SOCS3* in response to IFN-α2b stimulation (1000 IU/mL) for the indicated times. Repeat experiments n = 3-4. Data are presented as means ± SEMs (**P* < .05, ***P* < .01, 1-way ANOVA with Tukey correction for multiple comparisons). (**C**) STAT1 phosphorylation in response to IFN-γ after different IFN-α2b priming intervals.

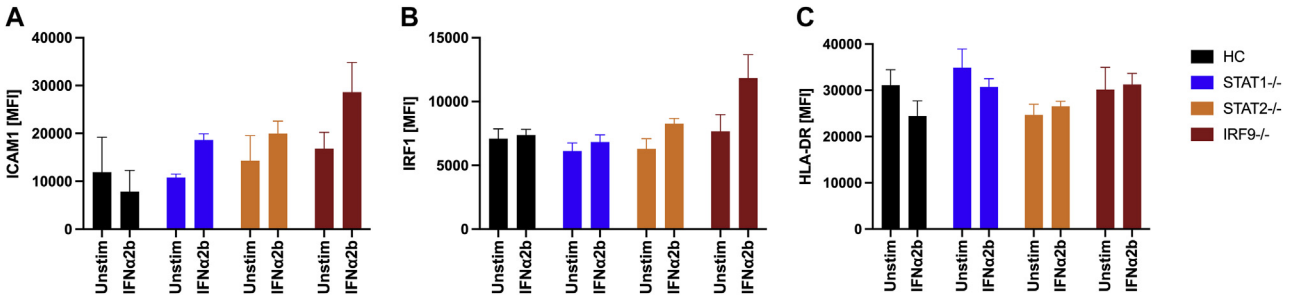

FIG E4. Expression of (**A**) ICAM1, (**B**) IRF1, and (**C**) HLA-DR in EBV-LCL after 48 hours of IFN-α2b stimulation (1000 IU/mL).

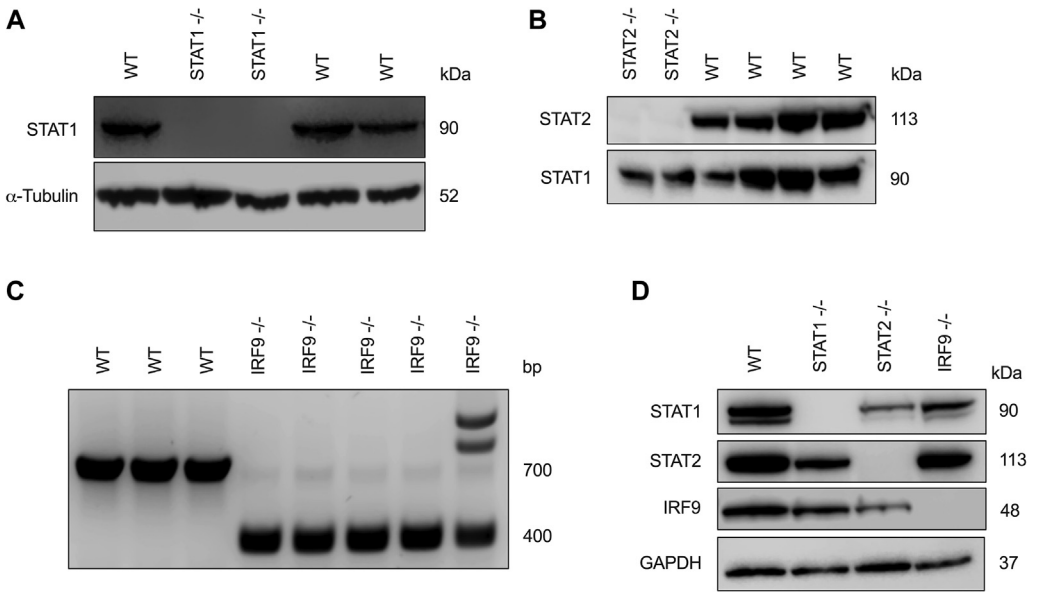

FIG E5. Verification of ISGF3 component knockouts in iPS-derived macrophages. Confirmation of complete knockout of (**A**) STAT1 and (**B**) STAT2 in iPS after gene editing. (**C**) *IRF9* sequence analysis of different iPS clones after gene editing since IRF9 protein expression could not be detected in iPS. (**D**) Complete absence of residual protein expression after differentiation into macrophages; number of repeat Western blot experiments in macrophages was 3.

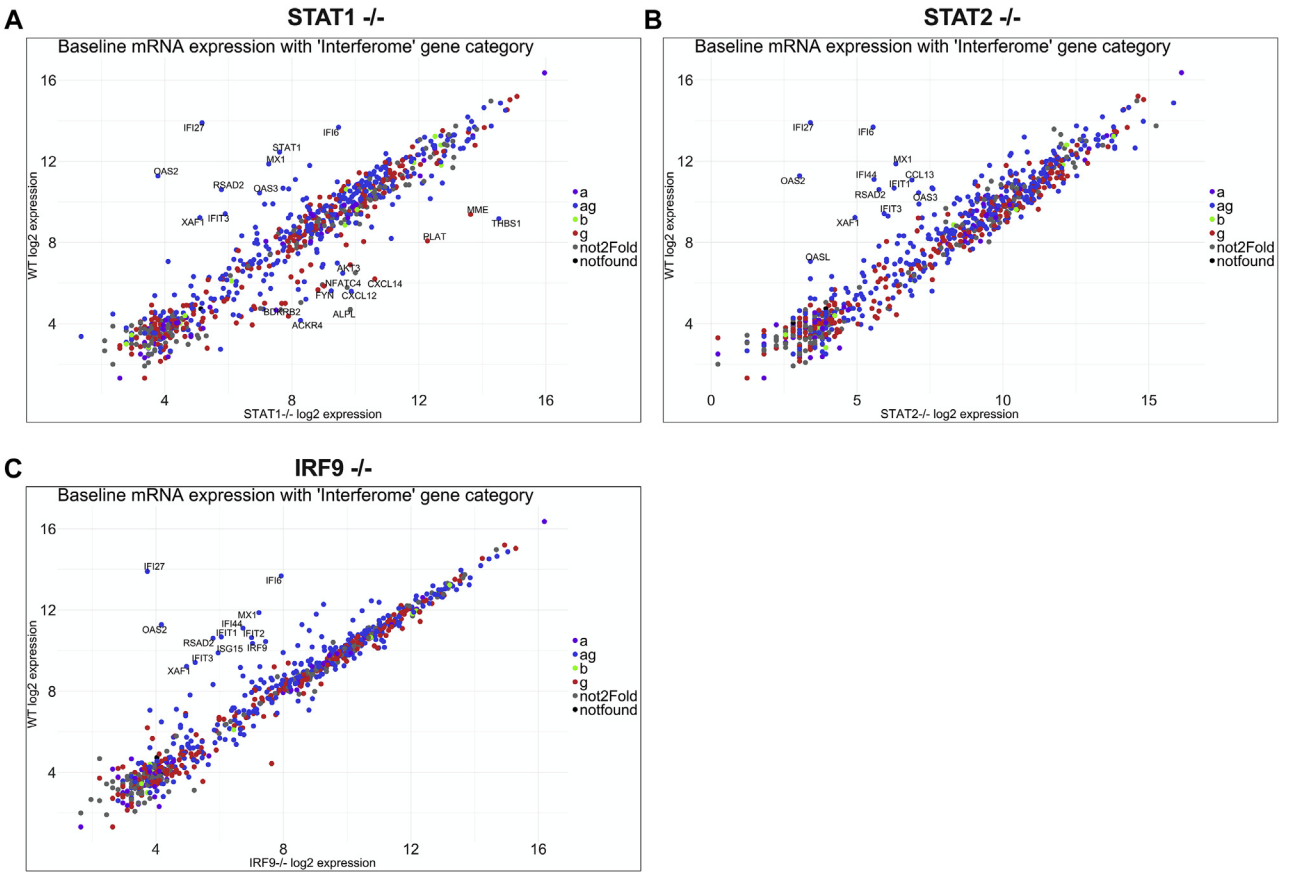

FIG E6. Differential gene expression at baseline in (**A**) STAT1$^{-/-}$, (**B**) STAT2$^{-/-}$, and (**C**) IRF9$^{-/-}$ iPS macrophages. Genes with a 10× increase or decrease compared to WT cells are labeled. Colors indicate the transcriptional influence of certain interferons based on the Interferome database v2.01 (Monash University, Australia), as follows: *purple,* IFN-α2b; *blue,* IFN-α2b and IFN-γ; *green,* IFN-β; *red,* IFN-γ; *gray,* not induced >2-fold; *black,* not found.

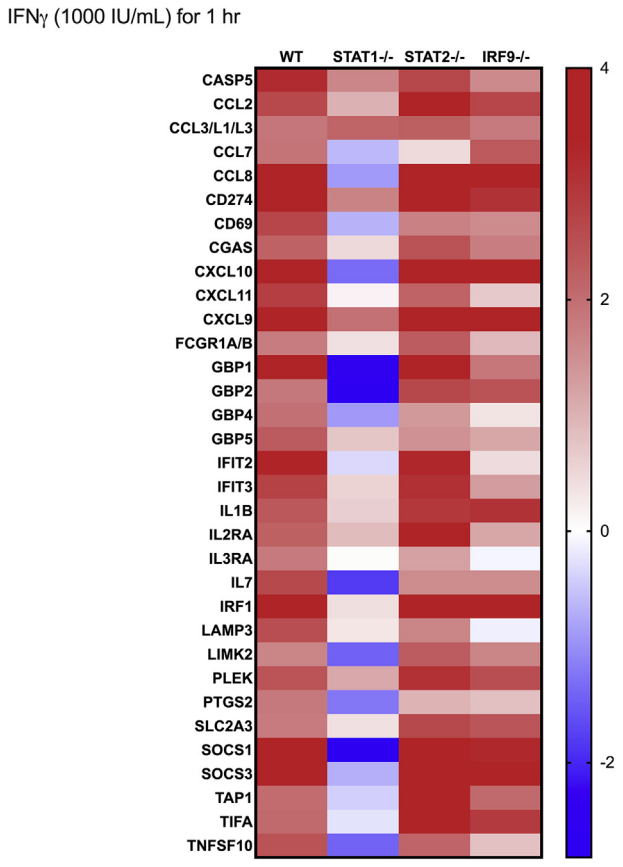

FIG E7. ISG induction after IFN-γ stimulation (1000 IU/mL) for 1 hour in WT, STAT1$^{-/-}$, STAT2$^{-/-}$, and IRF9$^{-/-}$ macrophages on an isogenic background. Only the genes with >1.5-fold induction in both WT lines are displayed.

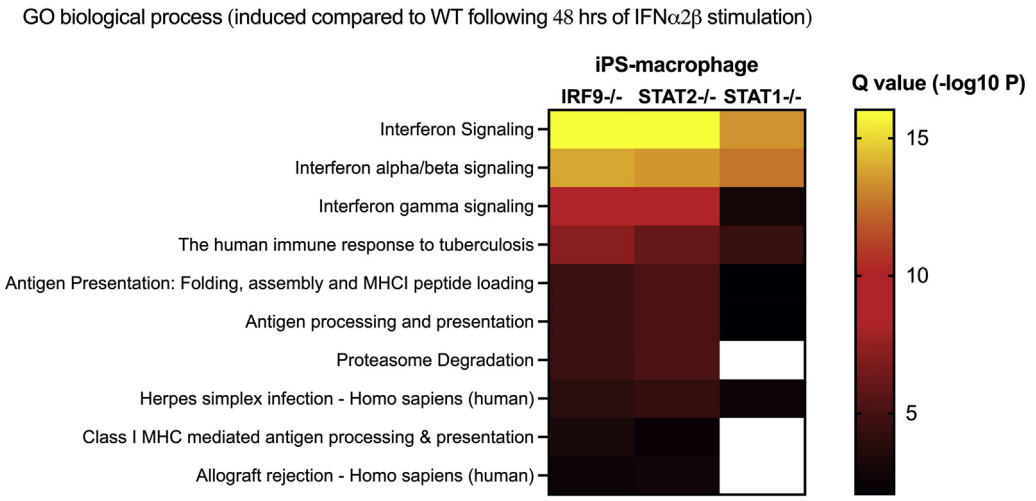

FIG E8. Pathway analysis after 48 hours of stimulation with IFN-α2b (1000 IU/mL), displaying the top 10 GO terms induced in STAT2$^{-/-}$ and IRF9$^{-/-}$ iPS macrophages.

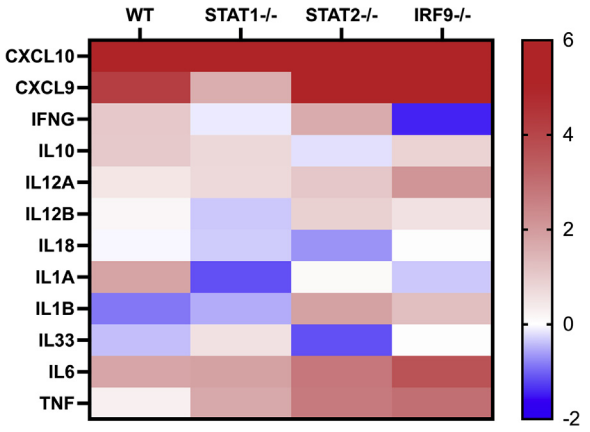

FIG E9. Transcriptional induction of cytokines relevant to HLH pathogenesis in iPS-derived macrophages stimulated with IFN-α2b (1000 IU/mL) for 48 hours.

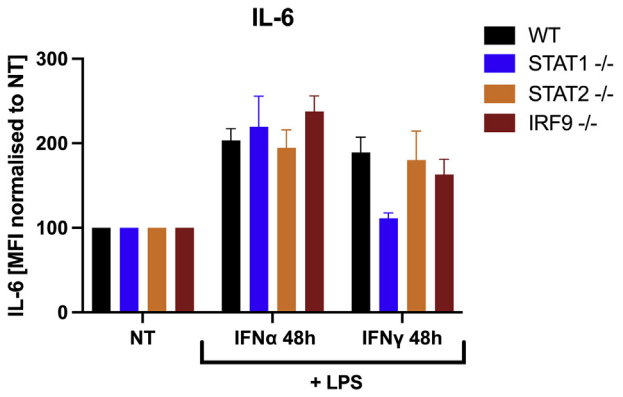

FIG E10. Intracellular IL-6 accumulation in iPS-derived macrophages primed for 48 hours with either IFN-α2b or IFN-γ (1000 IU/mL each) before being treated with lipopolysaccharide (LPS).

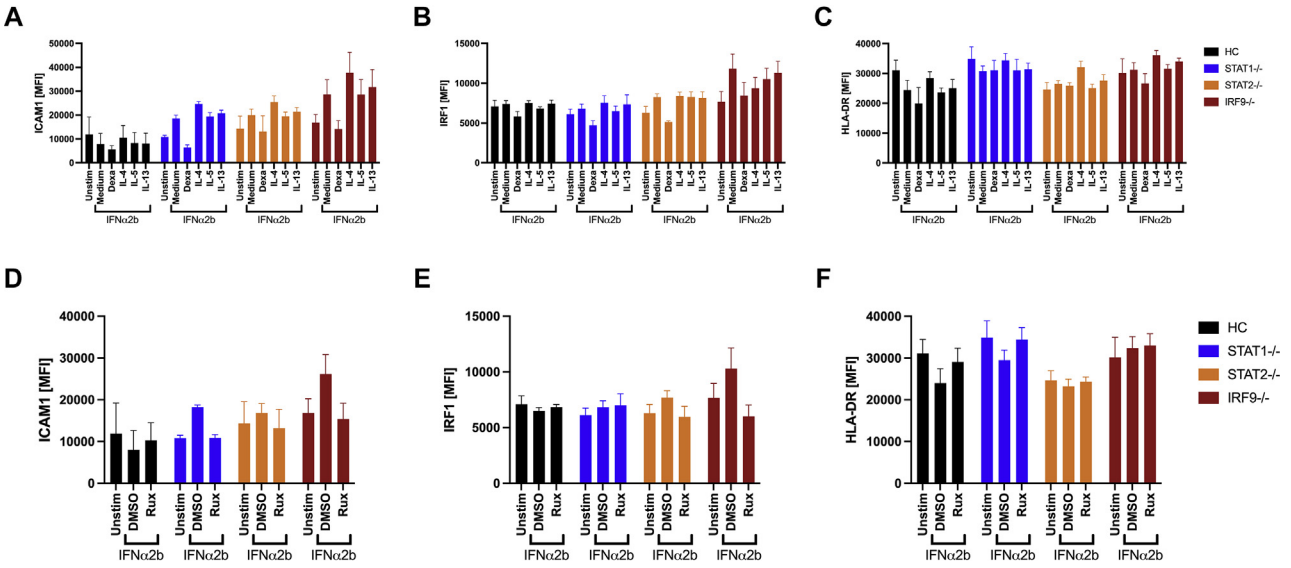

FIG E11. Expression of (**A**) ICAM1, (**B**) IRF1, and (**C**) HLA-DR in EBV-LCL pretreated with either IL-4, IL-5, or IL-15 (50 ng/mL each) or 10 μmol dexamethasone overnight before being stimulated with IFN-α2b (1000 IU/mL) for 48 hours. Blockade of type I IFN–induced upregulation of (**D**) *ICAM1,* (**E**) *IRF1,* and (**F**) HLA-DR expression by ruxotinib (1 μmol/L) pretreatment.

TABLE E1. Antibodies used for immunoblotting

Antibody	Host	Dilution	Source	Code
RSAD2	Rabbit	1:1000	CST	13996
ISG15	Rabbit	1:1000	CST	2743
STAT2	Mouse	1:2000	SCB	sc-1668
pSTAT2	Rabbit	1:2000	CST	8841
STAT1	Rabbit	1:1000	CST	9172
pSTAT1	Rabbit	1:1000	CST	7649
JAK1	Rabbit	1:500	CST	3344
pJAK1	Rabbit	1:500	CST	74129
MX1	Rabbit	1:1000	SCB	sc-50509
α-Tubulin	Mouse	1:10,000	CST	3873
GAPDH	Rabbit	1:10,000	CST	5174
IRF9	Rabbit	1:1000	CST	76684
USP18	Rabbit	1:1000	CST	4813
STAT1a	Mouse	1:100	SCB	sc-417
STAT2	Rabbit	1:5000	SCB	sc-476
Anti-rabbit HRP-conjugated	Goat	Various	CST	7074
Anti-mouse HRP-conjugated	Horse	Various	CST	7076

CST, Cell Signaling Technologies; *SCB*, Santa-Cruz Biotechnology.

TABLE E2. Antibodies used for PhosFlow

Antibody	Fluorophore	Host	Clone	Source	Code
p-STAT1	AF488	Mouse	4a	BD	612596
p-STAT2	AF647	Rabbit	D3P2P	CST	90740
Zombie UV				Biolegend	423107

TABLE E3. Primer sequences and probes used for qRT-PCR

Gene	Fwd sequence	Rev sequence	Probe ID
SOCS1	GCCCCTTCTGTAGGATGGTA	CTGCTGTGGAGACTGCATTG	87
SOCS3	CTTCGACTGCGTGCTCAA	GTAGGTGGCGAGGGGAAG	1
USP18	CAACGTGCCCTTGTTTGTC	ATCAGGTTCCAGAGTTTGAGGT	44
MX1	TGCATTGCAGAAGGTCAGAG	CCTCCATGGAAGAGTCTGTTG	11
RSAD2	GAGGGTGAGAATTGTGGAGAAG	GCGCTCCAAGAATCTTTCAA	9
IFI44L	TGACACTATGGGGCTAGATGG	TTGGTTTACGGGAATTAAACTGAT	15
IRF1	CAGATCTGAAGAACATGGATGC	ACAGGGAATGGCCTGGAT	20
ICAM1	GAAGTGGTGGGGGAGACATA	CCCAATAGGCAGCAAGTTTC	48
CIITA	CAGCTGTGCTCTGGACAGG	TGCTGAGGCTCATGGGATA	80
18S	CCGATTGGATGGTTTAGTGAG	AGTTCGACCGTCTTCTCAGC	81

TABLE E4. Guide RNA sequences used for gene editing in iPS cells

Gene	Guide RNA sequence
STAT1	GAGGUCAUGAAAACGGAUGG
STAT1	GCUUUUAGCAGCAGUUUAUG
IRF9	CAGCAACUGAUACACCUUGU
IRF9	GAGCUCAGAAGGGAUUAUGC
STAT2	AGCCCUUAAAUCCAGGAUCC

TABLE E5. Antibodies used for flow cytometry in iPS-derived macrophages

Antibody	Fluorophore	Host	Clone	Source	Code
CD71	APC	Mouse	CY1G4	Biolegend	334107
CD206	PE	Mouse	19.2	BD	555954
CD45	APC-H7	Mouse	2D1	BD	560178
CD11c	BV421	Mouse	B-ly6	BD	562561
HLA-DR	BV650	Mouse	L243	Biolegend	307650
CD163	BV711	Mouse	GHI/61	Biolegend	333630
CD11b	BV785	Mouse	ICRF44	Biolegend	301346
CD14	BUV737	Mouse	M5E2	BD	612763
HLA-DR	FITC	Mouse	L243	Biolegend	307604
ICAM1	BV711	Mouse	HA58	BD	564078
IRF1	PE	Mouse	20/IRF-1	BD	566322
TNFα	AF647	Mouse	MAb11	Biolegend	502916
Zombie UV				Biolegend	423107
7-AAD				Biolegend	420404
IL-6	PE	Mouse	AS12	BD	340527